# A Perspective on Multi-Source Energy Harvesting Technology Using Piezoelectric and Thermoelectric Materials

Narasimha Prasad[1], Wenjie Li[2,] Sumanta Kumar Karan[2], Subrata Ghosh[2], Rabeya Smriti[2], Bed Poudel[2,]

[1]NASA Langley Research Center, Hampton, VA

[2]Department of Materials Science and Engineering, The Pennsylvania State University, State College, PA 16801, USA

## ABSTRACT

Energy harvesting using various locally available energy sources such as vibration energy, heat, sound, or magnetic field have become attractive topics for supplying power to modular electronic devices making them run independently in extreme environments. In this paper, we will be discussing the perspectives on thermoelectric (TE) and piezoelectric materials and devices, and then the concept of multi-source energy harvester using piezoelectric and thermoelectric devices and integration of them into a reliable and independent power source. TE materials having low thermal conductivity and high figure-of-merit ($zT$) are developed to convert even a small temperature gradient efficiently into electrical energy with the state-of-the-art conversion efficiency of ~15% and output power of ~56 W from single device. The piezoelectric device architecture is configured using high performance piezoelectric ceramics (Cu-Mn-PIN-PMN-PT). These ceramics exhibit high piezoelectric coefficient with high mechanical quality factor and low dielectric loss factor. Using these piezoelectric materials, power density as high a 2 mW/cm$^2$ is demonstrated in 1-1.5 g vibration environments. The piezoelectric device is attached on the surface of TE module to capture both the vibration and thermal energy sources to realize dual mode energy harvester. The multi-energy transfer strategy opens opportunities for a future generation of wireless and modular electronic devices. These devices would be useful in powering wearable electronic devices, micro sensor chargers, etc. in extreme environmental conditions using body heat/thermal sources and induced motion/vibrations.

**Keywords:** Energy harvesting, thermoelectric, piezoelectric, piezoelectric ceramics, Cu-Mn-PIN-PMN-PT, wearable electronic devices, dual energy harvester

## 1. INTRODUCTION

Wireless energy harvesting technology presents a promising avenue for extending the operational lifespan of energy-constrained devices such as mobile electronics, implantable medical devices (IMDs), sensor networks and Internet of Things (IoT) devices. These technologies often face limitations due to onboard battery capacity or the complexity of wired connections. By integrating wireless power transfer with energy harvesting systems, these devices can be powered more sustainably and efficiently. Optical, thermal, magnetic, and acoustic energy conversion are particularly attractive for ambient energy harvesting due to their abundance and accessibility.

Among these energy harvesting technologies, thermoelectric (TE) power generators enable direct energy conversion from heat to electricity [1, 2]. Being solid-state energy conversion technique, it has advantages of reliability, simplicity, lightweight, compactness, and environmental friendliness [1, 3]. To make TE technology feasible, it requires significant improvement in conversion efficiency ($\eta$), which is jointly determined by the Carnot efficiency and the dimensionless figure of merit [4], $zT = S^2\sigma T/(k_L + k_E)$, where $S$ is the Seebeck coefficient, $\sigma$ is the electrical conductivity, $T$ is the absolute temperature, and $k_L$ and $k_E$ are the lattice and electronic thermal conductivities, respectively. Improving $zT$ of a TE material by simultaneous optimization of transport parameters is a major fundamental challenge since these parameters are heavily interdependent [5-11]. For energy generation applications achieving a high $\eta$, TE materials with high average $zT_{avg}$ (>1) in wide range of temperature are required [1]. TE power generation technologies may play a crucial role for harnessing the heat generated by high-speed aerial vehicles like jet engines, rockets, and hypersonic crafts. These technologies enhance fuel efficiency, reduce $CO_2$ emission, and supply vital power for critical flight systems such as control, navigation, and communications [6, 12-19]. Additionally, compact TE generators (TEGs)

can tap into flight-generated heat to offer on-the-spot power for sensors and electronics in remote locations, enabling wireless operations. For instance, the current reliance on thermal batteries and conventional power generators for hypersonic vehicle power is constrained by SWaP (size, weight, and power) limitations. In contrast, TEGs, with their solid-state design, present an ideal solution to meet SWaP requirements for efficient thermal energy harvesting. Recent advancements in TE materials, particularly in $zT$ and the design of highly efficient modules, have opened the door to efficient thermal energy harvesting solutions.

Table 1 outlines the key factors, spanning materials, devices, and systems that influence the performance of TE devices and systems, along with their elated governance. The $\eta$ of a TE device is contingent upon the materials' $zT$ and temperature difference it operates within. The maximum output power ($P_r$) is determined by the power factor ($PF$) of TE materials, the temperature differential, the size of materials, and thermal and electrical contact resistances. In the context of thermal energy harvesting in hypersonic vehicles, the performance metrics of SWaP are intricately linked with the device design, material's $zT$, and contact resistance.

*Table 1 The key factors that determine TE device and system performance and correlated governance.*

| **Factors** | | **Equation/Governance** | | **Correlation to system** |
|---|---|---|---|---|
| **Materials' zT** | $zT$ | $zT = \alpha^2 T/\rho\kappa$ | [1] | Power performance<br>Temperature limitation |
| **Device performance** | $\eta$ | $\eta = \frac{\Delta T}{T_h} \cdot \frac{\sqrt{1+zT_{avg}}-1}{\sqrt{1+zT_{avg}}+T_c/T_h}$ | [2]* | Power performance<br>Temperature limitation |
| | $P_r$ | $P_r = \frac{PF \cdot \Delta T^2 \cdot A}{4(n+L)\cdot(1+2rl_c/L)^2}$ | [3]* | SWaP<br>Temperature limitation |
| **Power density** | $\omega$ | $\omega = P_r/M$ | [4]* | SWaP<br>Temperature limitation |

*: $zT_{avg}$ is the average figure of merit of TE materials, and $\Delta T$ ($T_h$–$T_c$, where $T_h$ and $T_c$ are the hot- and cold-side temperatures, respectively) is the temperature gradient across the device. $r$= [κ]/2κ$_c$ and $n$= 4ρ$_c$/[ρ] are referred to as the thermal and electrical contact parameters, $A$ and $L$ are the cross-sectional area and thickness of TE materials, κ$_c$ is the effective thermal conductivity of the contact layer, ρ$_c$ is the contact electrical resistivity, and $l_c$ is the thickness of the contact layer. $M$ is the mass of TE device.

Piezoelectric materials are a class of substances that possess a remarkable property: they can generate an electric charge in response to mechanical stress or deformation, and vice versa [20, 21]. This unique property has found widespread applications in various fields, from sensors and actuators to energy harvesting and medical devices. The magnetoelectric and ultrasound-based methods of energy harvesting using piezoelectric materials offer higher efficiencies and power density, making them promising alternatives at low frequency range (in kHz range) [22, 23]. Magnetic field energy harvesting using magnetoelectric devices involves two steps in converting the AC magnetic field to mechanical strain (magnetostriction) and mechanical strain to electric potential (piezoelectricity) [24]. Magnetoelectric transducers offer a promising solution for low-frequency magnetic field energy harvesting with high power density and safer field levels, as they result in less absorption and heating, and greater penetration through different lossy media [22]. In the last decade, magneto-mechano-electric generators have gained attention for harvesting 50-60 Hz magnetic field energy using various materials such as PZT/Metglas, Textured Fe-Ga/SCMF PMN-PZ-PT, Ni/low-loss PMN-PZ-PT, Ni/PMN-PZ-PT, etc [24-27]. Most of the reported devices have been designed to operate under strong magnetic fields >500 μT and possess large dimensions due to low frequency resonance requirements. Small sized magnetoelectric energy harvesters have been explored using different piezoelectric materials for IoTs, biomedical applications such as endovascular stimulation, multisite stimulation, neurostimulator etc [28-31].

In this paper, we will introduce a brief progress on TE and piezoelectric materials and devices. For TE section, we will showcase the high performance and cost-effective materials, thermal stability of materials and devices, functional graded materials architecture, interface design approach, and adaptable high power device strategy. For piezoelectric section, we mainly focus on piezoelectric-based wireless energy harvesting using magnetic and ultrasound source and the proposed multi-source energy harvester concept.

## 2. THERMOELECTRIC-BASED ENERGY HARVESTER

### 2.1 High performance and cost-effective TE materials

Certain TE compounds, like PbTe, skutterudite, and $Mg_3Sb_2$, demonstrate promising $zT$ performance. However, they are generally limited to temperatures up to 400-500 °C. In medium-high temperature range, like for hypersonic applications, half-Heusler (hH) materials stand out as the most favorable choice due to their compatibility with high temperatures, excellent thermal stability, and robust mechanical strength [1, 12]. These attributes make them well-equipped to tackle the challenges posed by extreme temperatures and rapid thermal cycling [5, 12-15, 17, 19, 32-35]. Recent advancements in the $zT$ properties of hH alloys further bolster their potential for practical applications. Overall, hH-based TE devices offer the most cost-effective solution, featuring high power density, the highest W/g (aspect ratio), favorable raw materials cost in $/W, and exceptional mechanical and thermally robustness (**Table 2**) [36, 37].

*Table 2 Cost performance analysis of various TE power generation modules.*

| **Materials** | **$Bi_2Te_3$ - system** | **Skutterudite** | **Half-Heusler** |
|---|---|---|---|
| **Working Temperature** | 50 – 230 °C | 40 – 500 °C | > 500 °C |
| **Module size** | 40mm×45mm | 50mm×50mm | 42mm×43mm |
| **Power (W)** | 7.95 | 10.8 | 56 |
| **Power density (W/cm$^2$)** | 0.44 | 0.43 | 3.13 |
| **TE leg power density (W/cm$^2$)** | 1.6 | 1.05 | 9.73 |
| **TE materials (g)** | 3.97 | 30.7 | 6.37 |
| **Power (W)/g of TE** | 2.0 | 0.35 | 8.88 |
| **Raw materials cost ($/kg)** | 115 | 30 | 130 |
| **Raw material ($/W)** | 0.057 | 0.92 | 0.015 |
| **Reliability** | Stable up to 230 °C | 5% degradation in 1000 thermal cycles | <10% degradation in 1000 thermal cycles at 600 °C |
| **Materials strength (GPa)**[14] | ~0.2 | ~7 | ~10.3 |

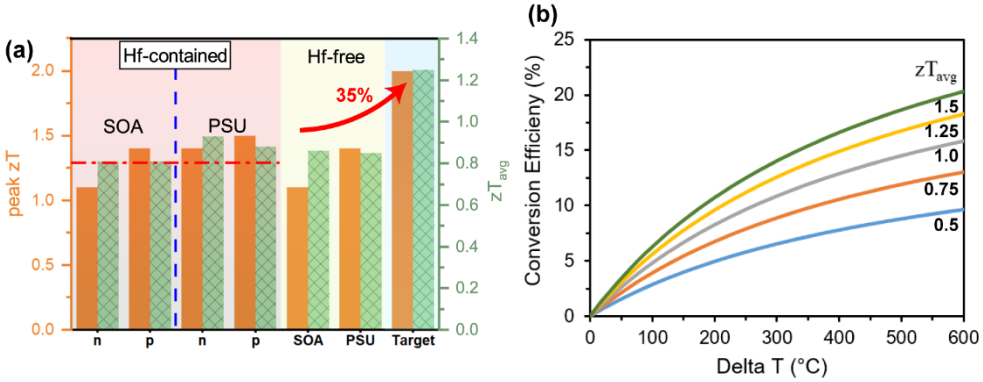


Figure 1 (a) The-state-of-the-art (SOA) $zT$ of Hf-contained and Hf-free hH TE materials and the next goal of materials (Target). PSU stands for the materials developed at Penn State University. (b) The relationship between $\Delta T$ and $\eta$ under different $zT_{avg}$.

The state-of-the-art (SOA) p-type hH compound, $(Nb_{0.88}Hf_{0.12})FeSb$ [12], shows a peak $zT$ of ~1.5 at 973 K and an average $zT$ ($zT_{avg}$) of 0.88 (ranging from 300-973 K). While for n-type hH alloy, $(Hf_{0.6}Zr_{0.4})NiSn_{0.99}Sb_{0.01}$ compound with tungsten nanoinclusions exhibits a peak $zT$ of 1.4 at 773 K and $zT_{avg}$ of 0.93 (ranging from 300-973 K) [5]. These accomplishments were achieved through innovative design strategies, focusing on defects, grain boundaries and nanoinclusions, resulting in significant advances compared to SOA results (Figure 1a). Towards practical application considerations, to achieve a $\eta$ of 20 % within a $\Delta T$ of 650 K, high-performance TE materials with a $zT_{avg}$ of 1.25 are necessary (Figure 1b). Nanostructured materials and high-entropy alloys (HEAs) offer a promising avenue to optimize both electrical and thermal properties in various TE materials, such as PbTe-based and GeTe-based alloys [38-41]. On the other hand, machine learning and density functional theory (DFT) approaches have predicted light elements, such as Mg, Ca, Al etc., as potential candidates for high-performance half-Heusler compounds [42]. A recent work reported a Hf-free MFeSb (M=Ta, Nb, Ti, V) half-Heusler materials with boasted $zT_{avg}$ exceeding 0.8 and a peak $zT$ of ~1.2 towards high power density thermal management [19].

## 2.2 Development of thermally stable and high strength compositions

The reliability, robustness and durability of TE devices and systems depend significantly on the thermal stability and mechanical properties of TE materials. These factors play a crucial role in minimizing the need for system maintenance, particularly in extreme environments. A deep understanding of these aspects is vital for the practical deployment of TE systems in such conditions. Previously, we explored the oxidation resistance and thermal stability of both half-Heusler-based materials and devices and succeeded in achieving stable materials and device performance up to 873 K in air and up to 1000 K in oxygen free environment. This was made by recognizing the importance of certain elements coexisting, which enabled the formation of binary intermetallic compounds and stable thin oxide layers. For example, the creation of a Nb-rich sublayer adjacent to the $TiO_2$ outer layer effectively prevented the migration of oxygen in a NbFeSb-based composition, resulting in stable electrical properties (

Figure 2a,b). As a result, the degradation of device output power was only 7 % after 7-days of operation at 873 K in air (

Figure 2c) [3]. Furthermore, we demonstrated excellent thermal stability of half-Heusler TE system after 1000 hours and 1000 cycles at 873 K (

Figure 2d,e) [43].

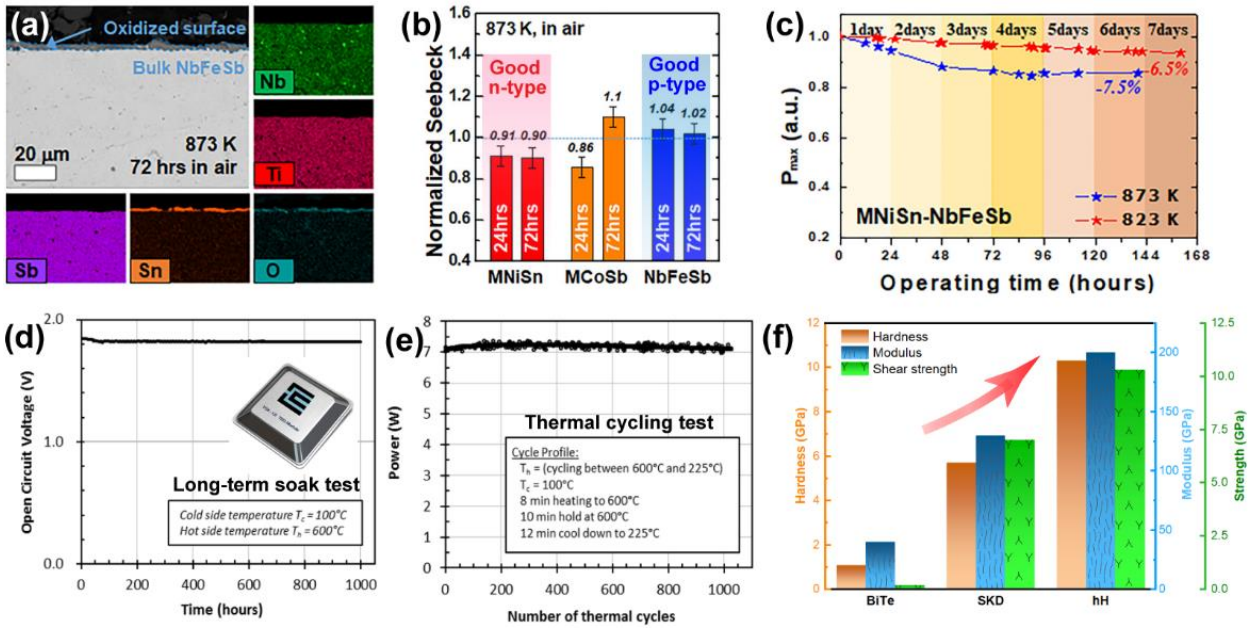


Figure 2 (a) SEM images of NbFeSb-based half-Heusler and (b) thermal stability of different half-Heusler compounds after exposing at 873 K in air [3]. (c) Normalized output power of half-Heusler device as a function of operation time [3]. Reproduced with permission from Kang et al [3]. Copyright 2020 American Chemical Society. (d) Long-term soaking test of hH devices and system [37]. (e) Thermal cycling test of hH devices and system [37]. (f) Comparison of mechanical properties in various TE materials.

TE materials with favorable mechanical properties are essential for device modules with extended service lifetimes, especially in conditions involving rapid thermal cycling. Vickers hardness exceeding 1 GPa and fracture toughness exceeding 1 MPa-$m^{1/2}$ are considered as a rough guideline for necessary mechanical properties in practical device applications [44]. Recent studies on high entropy hH compounds have shown superior Vickers hardness compared to both conventional hH and other TE materials (Figure 2 [32, 45]).

## 2.3 Functional Graded Materials (FGMs) device architecture

Conventional segmented TE devices face inherent limitations, which cap their conversion efficiency up to 12 % [17, 46-49]. These challenges stem from several key factors: 1) The substantial variations in densification temperatures

between the materials used in the segmented legs imposes restrictions on sintering them together. Consequently, these segments in the TE legs must be joined through soldering or brazing, using different materials. This results in heterogeneous interfaces leading to external electrical and thermal contact resistance, and relatively weak mechanical properties (Figure 3a). 2) The different segments exhibit significant differences in resistivity. When a load current passes through the entire segmented TE leg, a resistivity mismatch among the segments occurs. This means that various materials cannot be operated under their optimum conditions, resulting in performance lower than what would be expected from the combination of different material segments. This issue can be resolved through the design of FGMs. 3) According to the compatibility factor ($s$) theory [50], the difference in the optimum relative current density ($u$) among the segments restricts their efficient operation within a specific current magnitude range. When the difference in $s$ between these materials exceeds 2, it leads to a performance level that falls below expectations.

FGMs exhibit gradual variations in their compositions, structures, or properties throughout their volume. When designing FGMs for TE applications, the aim is to create spatially distributed electrical conductivity and Seebeck coefficients that ensure optimal temperature gradients across each material. This approach effectively overcomes issues related to resistivity and compatibility mismatch, while avoiding the presence of heterogeneous interfaces, all while maintaining a high $zT_{avg}$. Theoretically, the introduction of multi-layers materials can further boost $\eta$. Traditional contact electrode materials, such as Ni, have been commonly used in fabricating FGMs. However, their use can introduce heterogeneous interfaces, interdiffusion between the electrode and TE materials, and significant mismatches in the

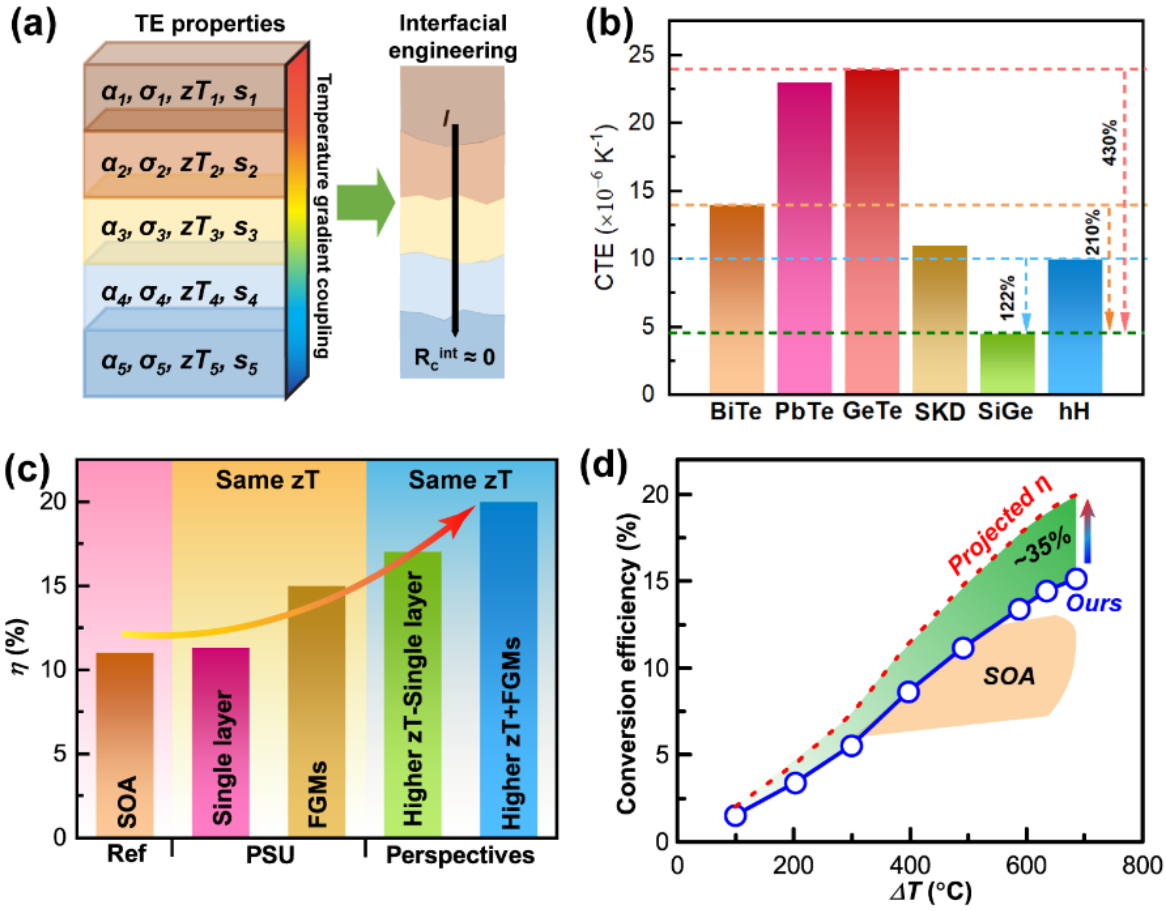


Figure 3 (a) FGMs design towards high device performance [12]. Reprinted with permission from Li et al [12]. Copyright 2023 Li et al. Distributed under the Creative Commons Attribution 4.0 License. (b) The typical CTE of various TE materials and their difference. Data calculated from reference [51-54]. (c) Conversion efficiency roadmap. PSU stands for the $\eta$ of TE devices developed at Penn State[12]. Perspectives refer to the next goal of $\eta$ potentially utilized by high zT and FGMs strategy. (d) Superior $\eta$ of ~15% of FGMS hH-based module compared to SOA results, and the future target of 20% $\eta$ by developing n-type FGMs hH TE materials.

coefficient of thermal expansion (*CTE*), which can vary widely among different TE materials, sometimes exceeding 400 % (Figure 3b) [51-54]. The benefits of FGMs design are substantial, leading to an approximate 36 % improvement in conversion efficiency when compared to single-layer modules using the same *zT* materials. This improvement can be further enhanced by combing FGMs design with higher *zT* materials (Figure 3c). A two-layers FGMs hH device, achieving a superior $\eta$ of 15.2 % for a single-leg module at a $\Delta T$ of 670 K (Figure 3c,d), has been reported [12]. Furthermore, the extensive compositional space offered by high entropy alloys design can expand the freedom of selection in FGMs, potentially satisfying multiple requirements in different aspects.

### 2.4 Interface design minimizing electrical and thermal contact resistance

Achieving high performance in a TE device requires not only a high $\Delta T$ and $zT_{avg}$ but also a critical focus on device design to minimize thermal and electrical contact resistances at the junction of metal electrode and TE leg (semiconductor). The electrical contact between metal and semiconductor can exhibit Schottky (rectifying) or ohmic (non-rectifying) behavior. In TE devices, ohmic contact behavior is essential for efficient electrical charge conduction and to reduce Joule heating [14]. Introducing a limited diffusion barrier at the junction of Cu electrode and TE legs is a practical way to control atomic diffusion, manage chemical reaction with TE materials, and maintain conductive electrical contact. However, such barriers can also create contact resistance, which can be exacerbated at high temperatures. In general, factors such as the choice of diffusion barrier material, the brazing technique and material used, and difference in *CTE* between TE legs and electrodes can contribute to high contact resistance This can lead to a deterioration of TE properties due to an extended diffused layer, reactions with TE materials at high temperature, and the generation and propagation of cracks at the junction during thermal cycling.

The device *ZT* ($ZT_d$) is critical in translating materials properties into TE device performance, which is defined as: $(ZT)_d = (ZT)_m \cdot \left(\frac{L}{L+2R_c\sigma}\right)$, where $(ZT)_m$ is materials' *zT*, $R_c$, *L*, and σ, which stand for contact resistance, the length of TE legs, and electrical conductivity of TE materials, respectively. The $R_c$ is getting more significant with the decrease of *L*. Therefore, the minimization of contact resistance in TE thin-profile device is the most critical challenge.

In past decades, different strategies to overcome the challenges of contact resistance in bulk TE devices have been developed [3, 13-15, 17]. For instance, a direct bonding technique for hH TE devices was developed, which demonstrated negligible contact resistance and clear interface, thereby achieving good TE performance with thermal stability (Figure 4a) [14]. An optimized Ti/Ni/Au coating layers were developed for metallization as the diffusion barrier and electrode contact layers, and the Cu–Sn transient liquid phase sintering technique is utilized for SKD and hH stages, which provides a high strength bonding and very low contact resistance (Figure 4b).[13]

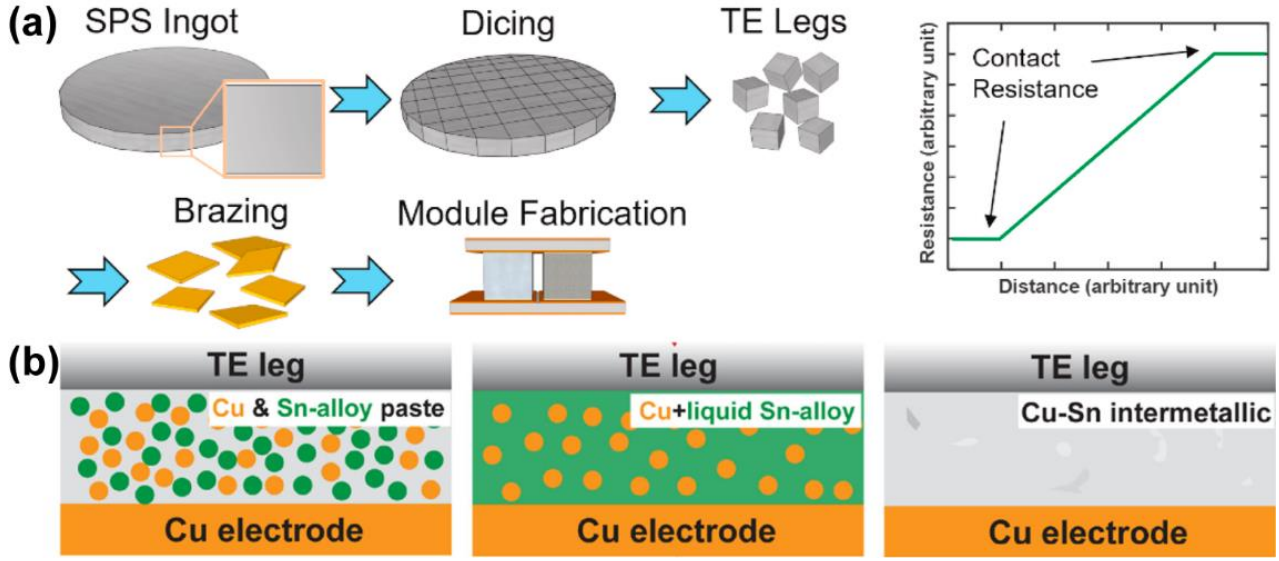


Figure 4 Metallization techniques of TE devices. (a) Direct bonding technique [14]. Reproduced with permission from Norzariasbmarz et al [14]. Copyright 2021 Elsevier. (b) Transient liquid phase sintering bonding technique. Reproduced with permission from Li et al [13]. Copyright 2023 American Chemical Society.

### 2.5 High power density and conformal TE device

In the context of TEGs, flexibility is of great importance for module integration into diverse architectural designs, including non-planar shapes like cylinders, which are commonly used in hypersonic vehicles and waste heat exhaust systems. Miniatured TEGs or flexible TEGs has been previously developed, primarily using materials like bismuth telluride or organic-based compounds. These have been tailored for low-temperature applications, such as body heat harvesting, to supply power in the microwatt to milliwatt range, facilitating self-powered batteries [55], but unsuitable for high temperature thermal energy harvesting [56, 57].

Recently, an innovative conformal module design, utilizing a strip-bridging technique to fabricate large-scale TE modules suitable for high temperature applications (Figure 5a). A superior output power of ~56 W within a 5×5 $cm^2$ device, resulting in a device power density ($\omega$) of 3.1 W/$cm^2$ (Figure 5b-d) [15]. The larger area of TE device, aimed at generating higher output power, leads to reduced heat fluxes ($Q_h$) across various hypersonic platforms. The conformal design allows for variable fill factor (*FF*) adjustments as needed, accommodating low $Q_h$ to achieve high $\eta$ and $\omega$ by maintaining a high hot-side temperature ($T_h$). This adaptability is not feasible with conventional rigid TEG module [15].

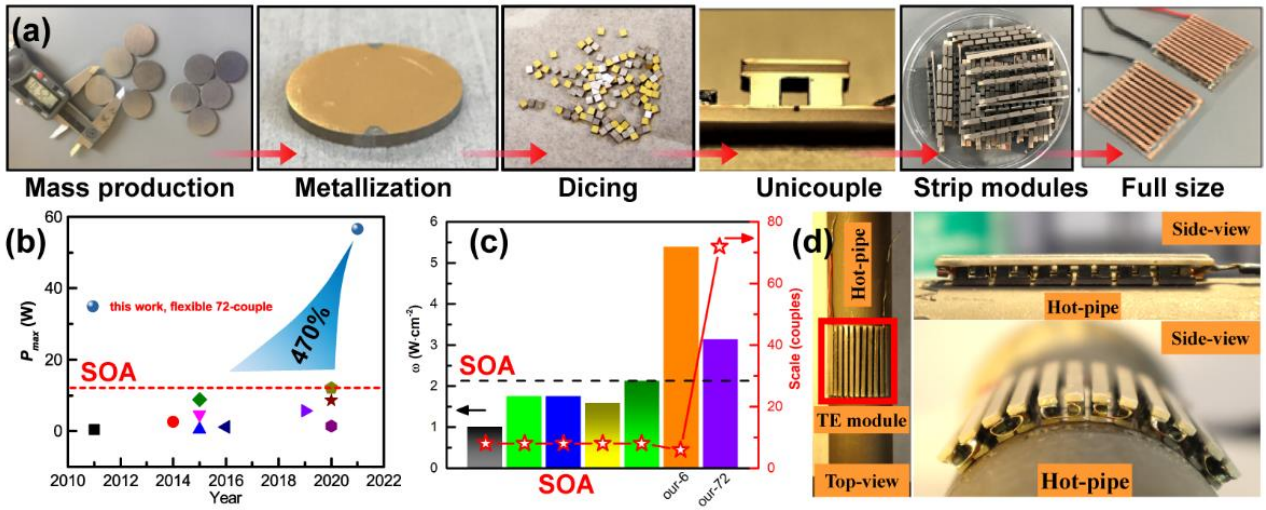


Figure 5 (a) Streamline TE device fabrication. Demonstration of large-scale conformal hH-based TE module: (b) Total output power and (c) device power density, (d) Module integrated on cylindrical hot-pipe. Reproduced with permission from Li et al [15]. Copyright 2021 American Chemical Society.

## 3. PIEZOELECTRIC-BASED ENERGY HARVESTER

### 3.1 Wireless Energy Harvesting using Magnetic and Ultrasound Source

Wireless power transfer technologies are being investigated and developed for application in IoTs and implantable devices [23, 29, 58-60]. Recently, a novel hybrid energy harvesting technology using both the ultrasound and magnetic energy under water/tissue (*ex-vivo*) mediums has been developed (Figure 6a,b) [61]. The newly designed hybrid device with disk architecture comprises of a high energy density novel $MnO_2$ and CuO co-doped $Pb(In,Nb)O_3$-$Pb(Mg,Nb)O_3$-$PbTiO_3$ (PIN-PMN-PT) piezoelectric disk-shaped transducer sandwiched between magnetostrictive Metglas layers. The magnetic field and ultrasound induced dual generator (MUDG) produces ultrahigh rms power of ~52.1 mW with power density of ~597 mW/$cm^3$ at ~500 μT magnetic field and 675 mW/$cm^2$ ultrasound intensity. This is the highest reported value compared to all the prior devices with applied input under safety limit (Figure 6c). Results demonstrate that MUDG can overcome the limitations of traditional wireless power systems for human body application, providing a new platform with the advantages of ultra-high-power density, small size, and tolerance to angular misalignment (x-y plane). Systematic studies including device optimization, the powering of electronics, transcutaneous transmission (Figure 6d), power transfer *ex-vivo*, and safety analysis, were conducted to evaluate its full potential for various applications.

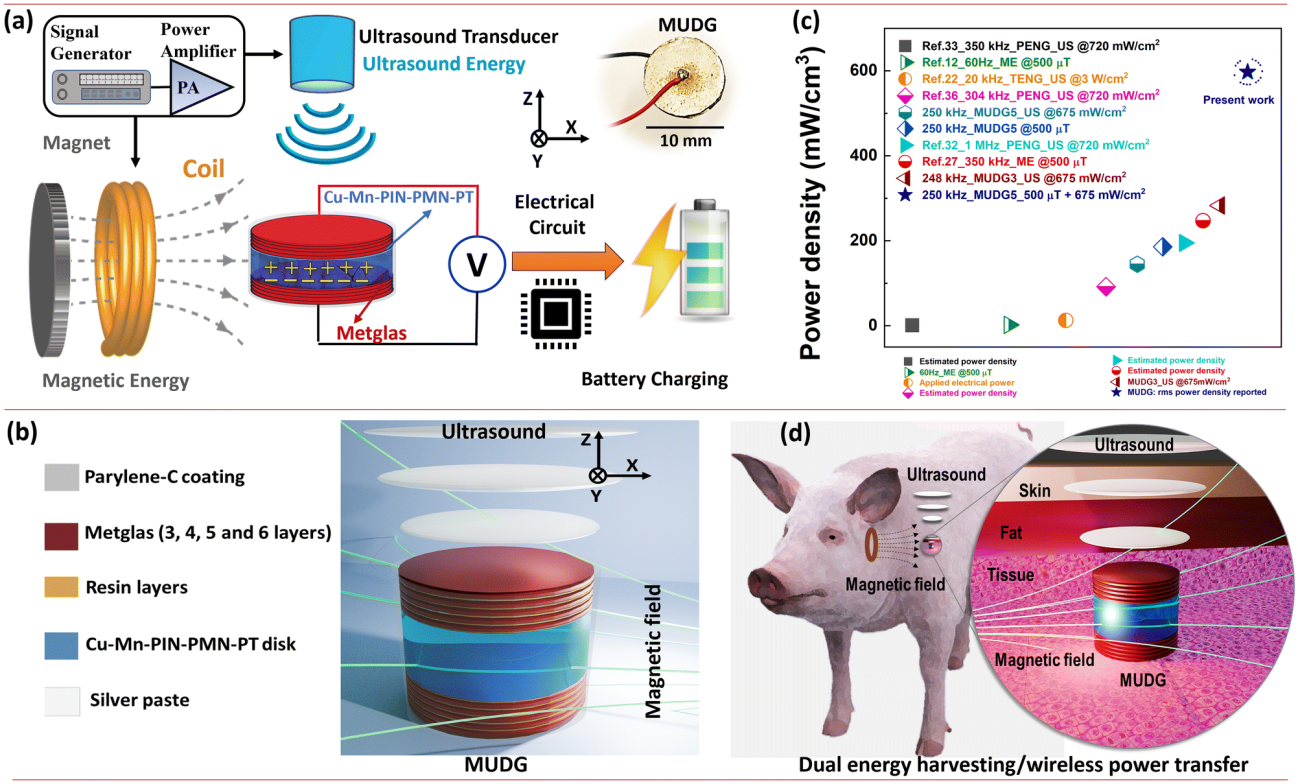


Figure 6 (a) The overview of the present work related to magnetic and ultrasound energy based dual energy harvesting and storage in a battery (inset shows real image of MUDG). (b) Schematic representation of the MUDG device for dual (magnetic field and ultrasound) energy harvesting with description of each component. (c) The comparison of power density of MUDG5 device with the other published technologies. (d) For the proof-of-concept experiments, the MUDG is implanted inside the porcine tissue and is wirelessly powered through magnetic field and ultrasound energy simultaneously. Reprinted with permission from Karan et al [61]. Copyright 2024 Karan et al. Distributed under the Creative Commons Attribution 3.0 License.

## 4. MULTI-SOURCE ENERGY HARVESTING

Utilizing multi-source energy harvesting technology in a single platform could be significant to improve the power performance towards wireless sensors and IoT devices of interest. A multi-source novel energy harvester design utilizing TE and piezoelectric energy harvesting technologies is discussed here. As shown in Figure 7, thermal energy harvesting utilizes the TE devices and magnetic and ultrasound energy is harvested using MUDG device.

For many applications, the thermoelectric device alone will be enough to power the wireless sensors requiring 10s of milliwatts of power. Even a relatively low temperature gradient of ~ 5 °C can consistently produce the power at 5 V needed to run most wireless sensors. However, the multi-source energy harvester would be useful to power sensors, which need higher voltages (> 10 V) to operate. Figure 7 illustrates the details of multi-source energy harvester design, which can utilize both energy sources (temperature gradient and vibrations) available in an aerial vehicles or other platforms. In this design, an essential part of the TE device (i.e. heat exchanger fins) is used as integrated piezoelectric devices. The heat exchange system made up of piezoelectric materials will be directly fabricated on the cold side of the thermoelectric module with an interdigitated electrodes pattern. The piezoelectric cantilevers are made in a sandwich structure with metglass/piezoelectric/metglass configuration.

Based on simulations, these hybrid harvesters can generate electrical power of as high as 500 mW at 5 °C temperature gradients, and 0.5–2 g and < 100Hz vibrations. This level of power output is enough to run most wireless sensors and IoT devices.

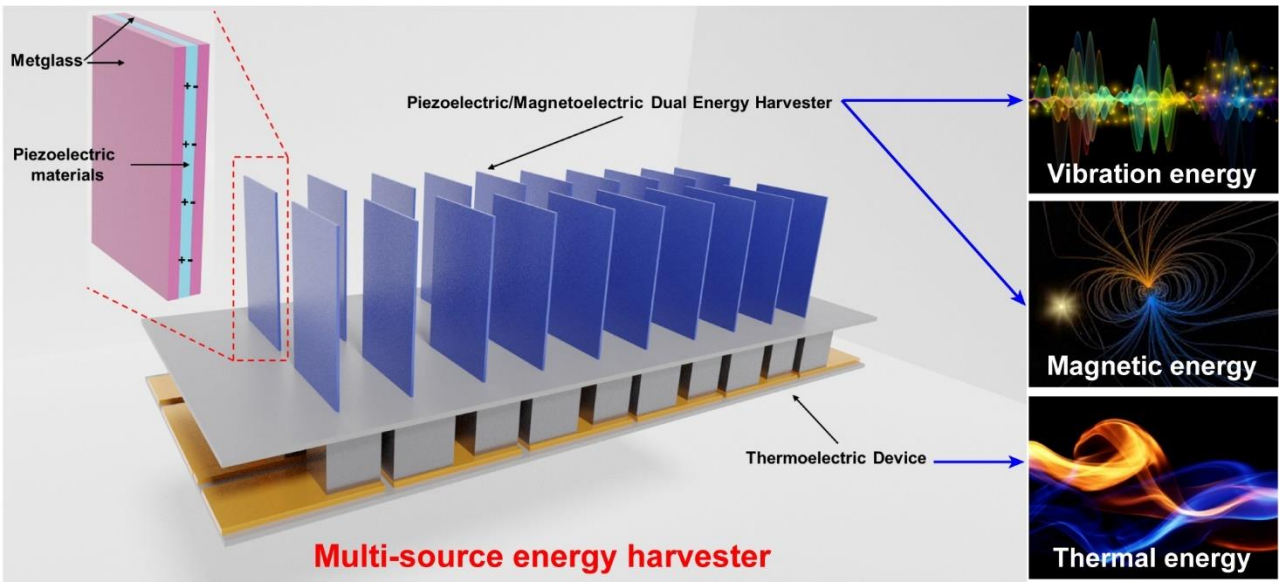

Figure 7 Concept of multi-source energy harvester by integrating TE device and piezoelectric/magnetoelectric devices. The details of piezoelectric cantilever can be found in Figure 6a.

## ACKNOWLEDGEMENTS

Penn State researchers acknowledge the financial support from the Army RIF program (contract number W911W6-19-C-0083).

## REFERENCES

[1] Wenjie Li, Subrata Ghosh, Na Liu *et al.*, "Half-Heusler thermoelectrics: Advances from materials fundamental to device engineering," Joule, 8, 1-38 (2024).

[2] Narasimha S Prasad *et al.*, "Development of PbTe material for advanced thermoelectric power generation." Proceedings Volume 8377, Energy Harvesting and Storage: Materials, Devices, and Applications III; 83770K (2012).

[3] H. B. Kang, U. Saparamadu, A. Nozariasbmarz *et al.*, "Understanding Oxidation Resistance of Half-Heusler Alloys for in-Air High Temperature Sustainable Thermoelectric Generators," ACS Appl. Mater. Inter., 12(32), 36706-36714 (2020).

[4] Narasimha S Prasad, *et al.*, "Inhomogeneous thermoelectric materials: improving overall zT by localized property variations." Proceedings Volume 9493, Energy Harvesting and Storage: Materials, Devices, and Applications VI; 949305(2015) .

[5] H. B. Kang, B. Poudel, W. Li *et al.*, "Decoupled Phononic-electronic Transportin Multi-phasen-type Half-Heusler Nanocomposites Enabling Efficient Hightemperature Power Generation," Mater. Today, 36, 63-72 (2020).

[6] G. Nie, W. Li, J. Guo *et al.*, "High Performance Thermoelectric Module Through Isotype Bulk Heterojunction Engineering of Skutterudite Materials," Nano Energy, 66, 104193 (2019).

[7] W. Li, J. Wang, Y. Xie *et al.*, "Enhanced Thermoelectric Performance of Yb-Single-Filled Skutterudite by Ultralow Thermal Conductivity," Chem. Mater., 31(3), 862-872 (2019).

[8] W. Li, J. Wang, B. Poudel *et al.*, "Filiform Metal Silver Nanoinclusions To Enhance Thermoelectric Performance of P-type $Ca_3Co_4O_{9+\delta}$ Oxide," ACS Appl. Mater. Inter., 11(45), 42131-42138 (2019).

[9] N. S. Prasad, T. Patrick, and N. David, "Shockwave consolidation of nanostructured thermoelectric materials." Proceedings of SPIE - The International Society for Optical Engineering 9226, 92260J.

[10] N. S. Prasad, J. T. Patrick, B. T. Sudhir *et al.*, "New technology for microfabrication and testing of a thermoelectric device for generating mobile electrical power." Proceedings Volume 7764, Nanoengineering: Fabrication, Properties, Optics, and Devices VII; 776409 (2010).
[11] Y. Zhang, Z. Li, S. Singh *et al.*, "Defect-Engineering-Stabilized $AgSbTe_2$ with High Thermoelectric Performance," Adv. Mater., 35(11), 2208994 (2023).
[12] W. J. Li, B. Poudel, R. A. Kishore *et al.*, "Toward High Conversion Efficiency of Thermoelectric Modules through Synergistical Optimization of Layered Materials," Adv. Mater., 35, 2210407 (2023).
[13] W. J. Li, G. K. Goyal, D. Stokes *et al.*, "High-Performance Skutterudite/Half-Heusler Cascaded Thermoelectric Module Using the Transient Liquid Phase Sintering Joining Technique," ACS Appl. Mater. Inter., 15, 2961−2970 (2023).
[14] A. Nozariasbmarz, U. Saparamadu, W. J. Li *et al.*, "High-performance half-Heusler thermoelectric devices through direct bonding technique," J. Power Sources, 493, 229695 (2021).
[15] W. Li, A. Nozariasbmarz, R. A. Kishore *et al.*, "Conformal High-Power-Density Half-Heusler Thermoelectric Modules: A Pathway toward Practical Power Generators," ACS Appl. Mater. Inter., 13(45), 53935-53944 (2021).
[16] A. Nozariasbmarz, B. Poudel, W. Li *et al.*, "Bismuth Telluride Thermoelectrics with 8% Module Efficiency for Waste Heat Recovery Application," iScience, 23(7), 101340 (2020).
[17] W. Li, B. Poudel, A. Nozariasbmarz *et al.*, "Bismuth Telluride/Half-Heusler Segmented Thermoelectric Unicouple Modules Provide 12% Conversion Efficiency," Adv. Energy Mater., 10(38), 2001924 (2020).
[18] W. Li, D. Stokes, B. Poudel *et al.*, "High-Efficiency Skutterudite Modules at a Low Temperature Gradient," Energies, 12(22), 4292 (2019).
[19] H. Zhu, W. Li, A. Nozariasbmarz *et al.*, "Half-Heusler alloys as emerging high power density thermoelectric cooling materials," Nat. Commun., 14, 3300 (2023).
[20] Y. K. Yan, K. H. Cho, and S. Priya, "Templated Grain Growth of ⟪001⟫-Textured 0.675Pb(MgNb)O-0.325PbTiO Piezoelectric Ceramics for Magnetic Field Sensors," J. Am. Ceram. Soc., 94(6), 1784-1793 (2011).
[21] Y. K. Yan, J. E. Zhou, D. Maurya *et al.*, "Giant piezoelectric voltage coefficient in grain-oriented modified PbTiO material," Nat. Commun., 7, (2016).
[22] S. Hosur, R. Sriramdas, S. K. Karan *et al.*, "A Comprehensive Study on Magnetoelectric Transducers for Wireless Power Transfer Using Low-Frequency Magnetic Fields," IEEE transactions on biomedical circuits and systems, 15(5), 1079-1092 (2021).
[23] R. Hinchet, H.-J. Yoon, H. Ryu *et al.*, "Transcutaneous ultrasound energy harvesting using capacitive triboelectric technology," Science, 365(6452), 491-494 (2019).
[24] H. Lee, R. Sriramdas, P. Kumar *et al.*, "Maximizing power generation from ambient stray magnetic fields around smart infrastructures enabling self-powered wireless devices," Energy & Environmental Science, 13(5), 1462-1472 (2020).
[25] V. Annapureddy, M. Kim, H. Palneedi *et al.*, "Low-loss piezoelectric single-crystal fibers for enhanced magnetic energy harvesting with magnetoelectric composite," Advanced Energy Materials, 6(24), 1601244 (2016).
[26] J. Ryu, J.-E. Kang, Y. Zhou *et al.*, "Ubiquitous magneto-mechano-electric generator," Energy & Environmental Science, 8(8), 2402-2408 (2015).
[27] V. Annapureddy, S.-M. Na, G.-T. Hwang *et al.*, "Exceeding milli-watt powering magneto-mechano-electric generator for standalone-powered electronics," Energy & Environmental Science, 11(4), 818-829 (2018).
[28] C. Chen, Z. Wen, J. Shi *et al.*, "Micro triboelectric ultrasonic device for acoustic energy transfer and signal communication," Nature communications, 11(1), 1-9 (2020).
[29] J. C. Chen, P. Kan, Z. Yu *et al.*, "A wireless millimetric magnetoelectric implant for the endovascular stimulation of peripheral nerves," Nature Biomedical Engineering, 1-11 (2022).
[30] Z. Yu, J. C. Chen, Y. He *et al.*, "Magnetoelectric Bio-Implants Powered and Programmed by a Single Transmitter for Coordinated Multisite Stimulation," IEEE Journal of Solid-State Circuits, (2021).
[31] Z. Yu, J. C. Chen, B. W. Avants *et al.*, "34.3 An 8.2 mm 3 Implantable Neurostimulator with Magnetoelectric Power and Data Transfer." 510-512.
[32] S. Ghosh, Y. Xia, A. Nozariasbmarz *et al.*, "High Entropy Engineering p-type Half-Heusler with High Thermoelectric Performance," unpublished data (2023).
[33] K. S. Kim, Y. M. Kim, H. Mun *et al.*, "Direct Observation of Inherent Atomic-Scale Defect Disorders responsible for High-Performance (TiHf)Ni(SnSb) Half-Heusler Thermoelectric Alloys," Adv. Mater., 29(36), 1702091 (2017).

[34] H. Zhu, R. He, J. Mao *et al.*, "Discovery of ZrCoBi based half Heuslers with high thermoelectric conversion efficiency," Nat. Commun., 9(1), 2497 (2018).
[35] J. J. Yu, C. G. Fu, Y. T. Liu *et al.*, "Unique Role of Refractory Ta Alloying in Enhancing the Figure of Merit of NbFeSb Thermoelectric Materials," Adv. Energy Mater., 8(1), 1701313 (2018).
[36] G. D. Li, Q. An, B. Duan *et al.*, "Fracture toughness of thermoelectric materials," Mat Sci Eng R, 144, 100607 (2021).
[37] B. Poudel, "Cost performance analysis of thermoelectric power generation modules," Evident Thermoelectric Inc.
[38] S. Ghosh, L. Raman, S. Sridar *et al.*, "High-Entropy Engineering in Thermoelectric Materials: A Review," Crystals, 14(5), 432 (2024).
[39] B. B. Jiang, Y. Yu, J. Cui *et al.*, "High-entropy-stabilized chalcogenides with high thermoelectric performance," Science, 371(6531), 830-834 (2021).
[40] B. B. Jiang, Y. Yu, H. Y. Chen *et al.*, "Entropy engineering promotes thermoelectric performance in p-type chalcogenides," Nat. Commun., 12(1), 3234 (2021).
[41] B. B. Jiang, W. Wang, S. X. Liu *et al.*, "High figure-of-merit and power generation in high-entropy GeTe-based thermoelectrics," Science, 377(6602), 208-213 (2022).
[42] H. Miyazaki, T. Tamura, M. Mikami *et al.*, "Machine learning based prediction of lattice thermal conductivity for half-Heusler compounds using atomic information," Sci. Rep., 11(1), 13410 (2021).
[43] A. S. Rao, G. Joshi, B. Poudel *et al.*, "A custom designed modular, scalable test system for an efficient performance evaluation of thermoelectric devices," Energ Convers Man-X, 14, 100228 (2022).
[44] Q. Y. Yan, and M. G. Kanatzidis, "High-performance thermoelectrics and challenges for practical devices," Nat. Mater., 21(5), 503-513 (2022).
[45] R. He, S. Gahlawat, C. F. Guo *et al.*, "Studies on mechanical properties of thermoelectric materials by nanoindentation," Phys. Status Solidi A, 212(10), 2191-2195 (2015).
[46] Y. Xing, R. Liu, J. Liao *et al.*, "A Device-to-Material Strategy Guiding the "Double-High" Thermoelectric Module," Joule, 4(11), 2475-2483 (2020).
[47] B. B. Jiang, X. X. Liu, Q. Wang *et al.*, "Realizing high-efficiency power generation in low-cost PbS-based thermoelectric materials," Energy Environ. Sci., 13(2), 579-591 (2020).
[48] P. H. Ngan, L. Han, and D. V. Christensen, "Joining of Half-Heusler and Bismuth Tellurides for Segmented Thermoelectric Generators," J. Electron. Mater., 47(1), 701-710 (2018).
[49] Q. H. Zhang, J. C. Liao, Y. S. Tang *et al.*, "Realizing a Thermoelectric Conversion Efficiency of 12% in Bismuth Telluride/Skutterudite Segmented Modules Through Full-parameter Optimization and Energy-loss Minimized Integration," Energy Environ. Sci., 10(4), 956-963 (2017).
[50] G. J. Snyder, and T. S. Ursell, "Thermoelectric efficiency and compatibility," Phys. Rev. Lett., 91(14), 148301 (2003).
[51] G. Schierning, R. Chavez, R. Schmechel *et al.*, "Concepts for medium-high to high temperature thermoelectric heat-to-electricity conversion: a review of selected materials and basic considerations of module design," Transl Mater Res, 2(2), (2015).
[52] D. A. Ferluccio, B. F. Kennedy, S. A. Barczak *et al.*, "Thermal properties of TiNiSn and VFeSb half-Heusler thermoelectrics from synchrotron x-ray powder diffraction," J Phys-Energy, 3(3), 035001 (2021).
[53] Y. I. Shtern, M. S. Rogachev, V. T. Bublik *et al.*, "The Results of Thermal Expansion Investigation for Effective Thermoelectric Materials," Ieee Nw Russ Young, 1932-1936 (2019).
[54] J. E. Ni, E. D. Case, R. D. Schmidt *et al.*, "The thermal expansion coefficient as a key design parameter for thermoelectric materials and its relationship to processing-dependent bloating," J. Mater. Sci., 48(18), 6233-6244 (2013).
[55] S. Q. Yang, P. F. Qiu, L. D. Chen *et al.*, "Recent Developments in Flexible Thermoelectric Devices," Small Sci, 1(7), 2100005 (2021).
[56] P. C. Zhu, Y. L. Wang, Y. Wang *et al.*, "Flexible 3D Architectured Piezo/Thermoelectric Bimodal Tactile Sensor Array for E-Skin Application," Adv. Energy Mater., 10(39), 2001945 (2020).
[57] S. J. Kim, H. E. Lee, H. Choi *et al.*, "High-Performance Flexible Thermoelectric Power Generator Using Laser Multiscanning Lift-Off Process," Acs Nano, 10(12), 10851-10857 (2016).
[58] M. Manoufali, K. Bialkowski, B. J. Mohammed *et al.*, "Near-field inductive-coupling link to power a three-dimensional millimeter-size antenna for brain implantable medical devices," IEEE Transactions on Biomedical Engineering, 65(1), 4-14 (2017).

[59] K. Wang, S. K. Karan, M. Sanghadasa *et al.*, “Implantable photoelectronic charging (I-PEC) for medical implants,” Energy Reviews, 100006 (2022).
[60] L. Jiang, Y. Yang, R. Chen *et al.*, “Flexible piezoelectric ultrasonic energy harvester array for bio-implantable wireless generator,” Nano energy, 56, 216-224 (2019).
[61] S. K. Karan, S. Hosur, Z. Kashani *et al.*, “Magnetic field and ultrasound induced simultaneous wireless energy harvesting,” Energy Environ. Sci., 17(6), 2129-2144 (2024).